Two-Dimensional ^{1}H NMR Studies on Octahedral Nickel(II) Complexes

Richard C. Holz,* Evgenij A. Evdokimov, and Feben T. Gobena

Department of Chemistry and Biochemistry, Utah State University, Logan, Utah 84322-0300

Received August 23, 1995[⊗]

The dinucleating ligand ethylene glycol−bis(β-aminoethyl ether) *N*,*N*,*N*′,*N*′-tetrakis[(2-(1-ethylbenzimidazoyl)] (EGTB-Et; **1**) was used to synthesize the dinuclear Ni(II) tetraacetonitrile complex cation $[Ni_2(EGTB\text{-}Et)(CH_3CN)_4]^{2+}$ (**2**): triclinic space group $P\bar{1}$ (a = 12.273(5) Å, b = 12.358(7) Å, c = 12.561(6) Å, α = 90.43(4)°, β = 110.26(3)°, γ = 99.21 (4)°, and Z = 1). The structure shows two identical octahedral Ni(II) centers each bound to two benzimidazole ring nitrogen atoms, one amine nitrogen atom, an ether oxygen atom, and two acetonitrile nitrogen atoms. The Ni(II) ions are tethered together by a diethyl ether linkage with a crystallographic center of inversion between the methylene carbons of this bridge. The Ni--Ni separation in **2** is 7.072 Å. The mononuclear Ni(II) complex cation $[Ni(Bipy)_2(OAc)]^+$ (**3**) (Bipy = bipyridine) was synthesized and crystallographically characterized: monoclinic space group $P2_1/c$ (a = 9.269(4) Å, b = 8.348(4) Å, c = 14.623(7) Å, and β = 102.46(4)°, Z = 2). The Ni(II) ions in **3** adopts a distorted octahedral geometry and is bound to four bipyridine ring nitrogen atoms and two carboxylate oxygen atoms. The average Ni−N and Ni−O distances are 2.062 and 2.110 Å. The electronic absorption spectra of both **2** and **3** were recorded in acetonitrile solution and are consistent with octahedral coordination geometries about the Ni(II) ions with Racah parameters of 840 and 820 cm^{-1}, respectively. Both one- and two-dimensional ^{1}H NMR techniques were used to assign the observed hyperfine shifted ^{1}H NMR resonances of **2** and **3** in acetonitrile solution. Clear COSY cross signals are observed between the aromatic protons of both the benzimidazole and pyridine protons of **2** and **3**, respectively. The use of 2D NMR methods to assign inequivalent aromatic protons rather than synthetic methods such as substitution or deuteration are discussed.

Introduction

Proton NMR spectroscopy has emerged as an excellent technique with which to probe the structural and magnetic properties of paramagnetic metal ions in both model complexes and biological systems.[1−3] Since only the protons proximate to the paramagnetic center are affected, a fingerprint of the metal ion environment can be obtained. These hyperfine-shifted resonances and their nuclear relaxation times are very sensitive to the distance and orientation of the proton to the paramagnetic metal ion. Thus, a wealth of structural and magnetic information can be obtained on the local environment of the paramagnetic metal center. However, a largely unexplored issue is the determination of the structural and magnetic properties of mono- and dinuclear Ni(II) ions in biological systems using two-dimensional ^{1}H NMR spectroscopy. Since high-spin Ni(II) ions exhibit fast electronic relaxation times (T_{1e}) that are sensitive to coordination number, relatively sharp hyperfine shifted ^{1}H NMR signals are observed, making Ni(II) an excellent spectroscopic probe.[1] In this regard, Ni(II) has been used as a replacement of the spectroscopically silent Zn(II) ion in enzymes such as Cu,Zn superoxide dismutase, carbonic anhydrase, and carboxypeptidase, to name a few;[2,5−8] however, relatively few two-dimensional ^{1}H NMR studies involving Ni(II) ions in either model complexes or biological systems have been reported.[6,9,10]

Several metalloenzymes such as urease, CO dehydrogenase, and several hydrogenases have now emerged that require Ni(II) ions for catalysis.[11] Of particular interest to us are the metallohydrolases with two or more metal ions making up a catalytic site. Urease is the only dinuclear hydrolase that utilizes Ni(II) as its native metal ion. Urease catalyzes the hydrolysis of urea to ammonia and carbamate, which in turn spontaneously decomposes to CO_2 and a second molecule of ammonia.[11] Of the remaining dinuclear hydrolases only the zinc dependent aminopeptidase from *Areomonas proteolytica* (AAP) has been reported to be reactivated by Ni(II). The addition of 2 equiv of Ni(II) to the apoenzyme hyperactivates AAP 25-fold compared to the native dizinc(II) enzyme.[12−14] To our knowledge, this is the only Zn(II) enzyme that can be hyperactivated by Ni(II). Since no physical or structural data for the Ni(II) substituted AAP enzyme has been reported, structural modifications leading to the hyperactivity of Ni(II)-substituted AAP are unknown.

Urease was recently crystallographically characterized and revealed a (μ-carbamato)dinickel(II) core.[15] One Ni(II) ion

[⊗] Abstract published in *Advance ACS Abstracts,* May 15, 1996.

(1) Bertini, I.; Luchinat, C. *NMR of Paramagnetic Molecules in Biological Systems*; Benjamin & Cummings: Menlo Park, CA, 1986.
(2) Bertini, I.; Turano, P.; Vila, A. J. *Chem. Rev.* **1993**, *93*, 2833−2932.
(3) La Mar, G. N.; de Ropp, J. S. *NMR Methodology for Paramagnetic Proteins*; Plenum Press: New York, 1993; Vol. 12, pp 1−78.
(4) Cheng, H.; Markely, J. L. *Annu. Rev. Biophys. Biomol. Struct.* **1995**, *24*, 209−237.
(5) Bertini, I.; Donaire, A.; Monnanni, R.; Moratal, J.-M.; Salgado, J. *J. Chem. Soc., Dalton Trans.* **1992**, 1443−1447.
(6) Bertini, I.; Luchinat, C.; Ming, L.-J.; Piccioli, M.; Sola, M.; Valentine, J. S. *Inorg. Chem.* **1992**, *31*, 4433−4435.
(7) Ming, L.-J.; Valentine, J. S. *J. Am. Chem. Soc.* **1990**, *112*, 6374−6383.
(8) Moratal, J. M.; Martinez-Ferrer, M.-J.; Jimenez, H. R.; Donaire, A.; Castells, J.; Salgado, J. *J. Inorg. Biochem.* **1992**, *45*, 231−241.
(9) Luchinat, C.; Steuernagel, S.; Turano, P. *Inorg. Chem.* **1990**, *29*, 4351−4353.
(10) Moratal, J.-M.; Salgado, J.; Donaire, A.; Jimenez, H. R.; Castells, J. *J. Chem. Soc., Chem. Commun.* **1993**, 110−112.
(11) Hausinger, R. P. *Biochemistry of Nickel*; Plenum Press: New York, 1993; Vol. 12, pp 23−180.
(12) Prescott, J. M.; Wagner, F. W.; Holmquist, B.; Vallee, B. L. *Biochem. Biophys. Res. Commun.* **1983**, *114*, 646−652.
(13) Prescott, J. M.; Wagner, F. W.; Holmquist, B.; Vallee, B. L. *Biochemistry* **1985**, *24*, 5350−5356.
(14) Bayliss, M. E.; Prescott, J. M. *Biochemistry* **1986**, *25*, 8113−8117.
(15) Jabri, E.; Carr, M. B.; Hausinger, R. P.; Karplus, P. A. *Science* **1995**, *268*, 998−1004.

S0020-1669(95)01106-2 CCC: $12.00

adopts a distorted tetrahedral geometry with two histidine ligands while the second is pentacoordinate with three histidine ligands. Before activation of urease with CO_2, the two Ni(II) ions are not spin-coupled but remain close enough to provide for bridging ligands.[11] The histidine-rich coordination geometry observed for urease is typical of mononuclear zinc hydrolases since most, such as those found in carboxypeptidases and endopeptidases, are histidine rich.[16] On the other hand, three aminopeptidases have been crystallographically characterized and reveal carboxylate-rich coordination environments. AAP contains a (μ-aqua)(μ-carboxylato)dizinc(II) core with one terminal chelated carboxylate and one histidine residue at each metal ion.[17] Both Zn(II) ions in AAP appear to be in a distorted trigonal bipyramidal coordination geometry with a Zn−Zn distance of 3.5 Å. Similarly, bovine lens leucine aminopeptidase contains a bis(μ-carboxylato)dizinc(II) core[18,19] with terminal carboxylate residues, while methionine aminopeptidase from *Escherichia coli* contains a bis(μ-carboxylato)dicobalt(II) core.[20] The histidine-rich coordination environment of urease compared to the carboxylate-rich coordination environments of aminopeptidases likely regulates the specific catalytic properties of each of these dinuclear hydrolases.

In an effort to gain insight into the use of two-dimensional ^{1}H NMR spectroscopy on octahedral Ni(II) centers in enzymes and carboxylate chelation to Ni(II) centers, we have designed and synthesized a new dinucleating ligand ethylene glycol−bis(β-aminoethyl ether) *N*,*N*,*N*′,*N*′-tetrakis[(2-(1-ethylbenzimidazoyl)] (EGTB-Et (**1**)). Transition metal complexes of **1** are

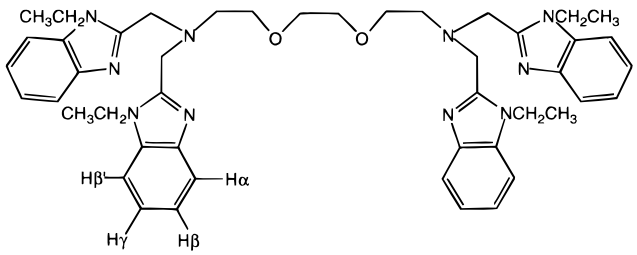

EGTB-Et
1

of interest since they will have "open" type structures with biologically relevant benzimidazole ligands.[21] Reaction of $Ni(ClO_4)_2{\cdot}6H_2O$ with **1** provides $[Ni_2(EGTB\text{-}Et)(CH_3CN)_4](ClO_4)_4{\cdot}2CH_3CN$ (**2**) which was crystallographically characterized. In addition, we have synthesized and crystallographically characterized $[Ni(Bipy)_2(OAc)]ClO_4{\cdot}2H_2O$ (**3**) (Bipy = bipyridine). Both of these complexes have been characterized by electronic absorption spectroscopy and both one- and two-dimensional (COSY) ^{1}H NMR techniques.

Experimental Methods

Synthetic Methods. All chemicals were purchased commercially and used as received. The dinucleating ligand ethylene glycol−bis(β-aminoethyl ether) *N*,*N*,*N*′,*N*′-tetrakis[(2-(1-ethylbenzimidazoyl)] (EGTB-Et; **1**) was synthesized by condensing 1,2-diaminobenzene with ethylene glycol−bis(β-aminoethyl ether) *N*,*N*,*N*′,*N*′-tetraacetic acid according to the method of McKee *et al.*[22] with minor revisions as previously reported.[21] Briefly, 1,2-diaminobenzene (5.27 g, 0.048 mol) and ethylene glycol−bis(β-aminoethyl ether) *N*,*N*,*N*′,*N*′-tetraacetic acid (4.61 g, 0.012 mol) were finely ground together and heated to 180−190 °C for 1 h. The resulting red glass was dissolved in 4 M HCl and heated to reflux with activated charcoal for 30 min. Upon filtration, the colorless liquid was neutralized with dilute sodium hydroxide. The resulting white solid was thoroughly dried and ground to a fine powder (6.4 g, 80%). N-alkylation was achieved by the method of Kikugawa *et al.*[23] The identity of EGTB-Et was confirmed by ^{1}H NMR spectroscopy. ^{1}H NMR ($CDCl_3$: δ 7.24): EGTB-Et d 1.31 (t, 12 H), 2.92 (t, 4 H), 3.45 (s, 4 H), 3.56 (t, 4 H), 3.95 (q, 8 H), 4.08 (s, 8 H), 7.19 (m, 8 H), 7.67 (m, 8 H).

Caution! *Perchlorate salts of transition metal complexes are potentially explosive. These complexes should be prepared only in small quantities and handled with care.*

The preparation of $[Ni_2(EGTB\text{-}Et)(CH_3CN)_4](ClO_4)_4{\cdot}2CH_3CN$ (**2**) is as follows: EGTB-Et (0.77 g; 1.0 mmol) was dissolved in 20 mL of methanol. To this solution 0.74 g (2.0 mmol) of $Ni(ClO_4)_2{\cdot}6H_2O$ dissolved in 2 mL of methanol was added. A blue precipitate resulted immediately and was collected by filtration. This solid was dissolved in acetonitrile and recrystallized by vapor diffusion with diethyl ether, yielding suitable crystals for X-ray crystallographic studies. Removal of the prismatic crystals from solution and drying in air resulted in the loss of an acetonitrile molecule from the crystal lattice and the uptake of two water molecules, forming $[Ni_2(EGTB\text{-}Et)(CH_3CN)_4](ClO_4)_4{\cdot}CH_3CN{\cdot}2H_2O$ (**2a**). The analytical purity of **2a** was checked by elemental analysis (Atlantic Microlab, Inc.). Anal. Calcd for $[Ni_2(EGTB\text{-}Et)(CH_3CN)_4](ClO_4)_4{\cdot}CH_3CN{\cdot}2H_2O$ (**2a**) ($C_{56}H_{75}N_{15}O_{20}Cl_4Ni_2$): C, 43.73; H, 4.90; N, 13.66. Found C, 43.78; H, 5.11; N, 13.41.

The preparation of $[Ni(Bipy)_2(OAc)]ClO_4{\cdot}2H_2O$ (**3**) is as follows: To a stirred methanol solution (20 mL) containing $Ni(CH_3CO_2)_2{\cdot}4H_2O$ (0.25 g; 1.0 mmol) was added 2,2′-bipyridine (Bipy) (0.18 g; 1.0 mmol). After 30 min, $NaClO_4$ (0.20 g) was added. This mixture was cooled to 4 °C and pink prismatic, X-ray quality crystals of **3** were deposited within 1 week. Removal of the prismatic crystals from solution and drying in air resulted in the loss of the water molecules from the crystal lattice. The analytical purity of **3** was checked by elemental analysis (Atlantic Microlab, Inc.). Anal. Calcd for $[Ni(Bipy)_2(OAc)]ClO_4$ (**3**) ($C_{22}H_{19}N_4O_6ClNi$): C, 49.89; H, 3.59; N, 10.58. Found C, 49.83; H, 3.67; N, 10.61.

Crystallographic Studies. Suitable crystals of **2** and **3** were selected and mounted in 0.5 mm diameter X-ray capillary tubes and centered optically on a Seimens P4 diffractometer equipped with an LT-2a low-temperature device that maintained the crystal at −100 °C throughout data collection. Autocentering of 25 reflections indicated monoclinic cells for both **1** and **2**. Systematic absences in the data set led to the unambiguous selection of the space groups $P\bar{1}$ and $P2_1/c$ for **2** and **3**, respectively. Two standard reflections were measured every 50 reflections and remained constant (±1%) throughout both data collections. The nickel atoms were located by direct methods and the remaining non-hydrogen atoms were located by subsequent difference maps and refined anisotropically. Hydrogen atoms were generated in idealized positions with fixed thermal parameters (0.08). A summary of the crystallographic data collection for **2** and **3** is presented in Table 1. The complete listing of the crystallographic data of both **2** and **3** is provided in the Supporting Information.

Physical Methods. Electronic absorption spectra were recorded on a Shimadzu UV-3101PC spectrophotometer. Elemental analyses were performed by Atlantic Microlabs, Inc. (Norcross, GA). All ^{1}H NMR spectra were recorded on a Bruker ARX-400 spectrometer. Chemical shifts (in ppm) are reported with respect to the residual solvent signal. Longitudinal relaxation times (T_1) were measured by the use of an inversion-recovery pulse sequence (180°−τ−90°). Plots of $\ln(I_o - I_\tau)$ vs τ for each signal are linear over all τ values investigated. Magnitude ^{1}H COSY spectra were obtained at 400.13 MHz on **2** and **3** in CD_3CN solutions. The COSY spectra were obtained at 40 and 10 °C for **2** and **3**, respectively. These spectra were typically obtained with 512 blocks

(16) Vallee, B. L.; Auld, D. S. *Biochemistry* **1990**, *29*, 5647−5659.
(17) Chevrier, B.; Schalk, C.; D'Orchymont, H.; Rondeau, J.-M.; Moras, D.; Tarnus, C. *Structure* **1994**, *2*, 283−291.
(18) Burley, S. K.; David, P. R.; Taylor, A.; Lipscomb, W. N. *Proc. Natl. Acad. Sci. U.S.A.* **1990**, *87*, 6878−6882.
(19) Burley, S. K.; David, P. R.; Sweet, R. M.; Taylor, A.; Lipscomb, W. N. *J. Mol. Biol.* **1992**, *224*, 113−140.
(20) Roderick, S. L.; Matthews, B. W. *Biochemistry* **1993**, *32*, 3907−3912.
(21) Holz, R. C.; Gobena, F. T. *Polyhedron*, in press.
(22) McKee, V.; Zvagulis, M.; Dagdigian, J. V.; Patch, M. G.; Reed, C. A. *J. Am. Chem. Soc.* **1984**, *106*, 4765−4772.
(23) Kikugawa, Y. *Synthesis* **1981**, 124−125.

Table 1. Summary of Crystallographic Data for $[Ni_2(EGTB\text{-}Et)(CH_3CN)_4](ClO_4)_4\cdot 2CH_3CN$ (**2**) and $[Ni(Bipy)_2(OAc)]ClO_4\cdot 2H_2O$ (**3**)

parameter	$[Ni_2(EGTB\text{-}Et)(CH_3CN)_4](ClO_4)_4\cdot 2CH_3CN$	$[Ni(Bipy)_2(OAc)]ClO_4\cdot 2H_2O$
chem formula	$C_{58}H_{74}N_{16}O_{18}Cl_4Ni_2$	$C_{22}H_{23}N_4O_8ClNi$
fw	1541.4	565.2
cryst syst	triclinic	monoclinic
space group	$P\bar{1}$	$P2_1/c$ (No. 14)
a (Å)	12.273(5)	9.269(4)
b (Å)	12.358(7)	8.348(4)
c (Å)	12.561(6)	14.623(7)
α (deg)	90.43(4)	90
β (deg)	110.26(3)	102.46(4)
γ (deg)	99.21(4)	90
V (Å^3)	1760.0(15)	1104.8(9)
Z	1	2
ρ_{calc} (g cm^{-3})	1.455	1.592
μ (mm^{-1})	0.765	1.071
radiation	Mo Kα ($\lambda = 0.710\ 73$ Å)	Mo Kα ($\lambda = 0.710\ 73$ Å)
temp (°C)	−100	−100
residuals:[a] R; R_w	0.066; 0.074	0.048; 0.073

[a] $R = \sum||F_o| - |F_c||/\sum|F_o|$; $R_w = [(\sum w(|F_o| - |F_c|)^2/\sum wF_o^2)]^{1/2}$; $w = 1/\sigma^2(|F_o|)$.

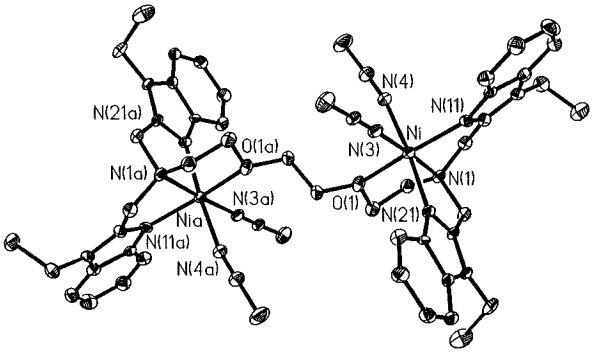

Figure 1. ORTEP drawing of the $[Ni_2(EGTB\text{-}Et)(CH_3CN)_4]^{4+}$ cation showing a partial numbering scheme (carbon and hydrogen atoms are not labeled for clarity).

of 1024 complex points. An unshifted sine−bell-squared weighting function was applied prior to Fourier transformation followed by baseline correction in both dimensions and symmetrization.

Results and Discussion

Structural Studies. X-ray diffraction studies were carried out on $[Ni_2(EGTB\text{-}Et)(CH_3CN)_4](ClO_4)_4\cdot 2CH_3CN$ (**2**). Compound **2** crystallizes in the triclinic space group $P\bar{1}$. One $[Ni_2(EGTB\text{-}Et)(CH_3CN)_4]^{4+}$ cation is found in the unit cell along with four perchlorate anions and two acetonitrile molecules. The packing diagram of **2** indicates that the benzimidazole rings of one cation stack with the benzimidazole rings of a second molecule (see Supporting Information). A thermal ellipsoid drawing of the cation of **2** with a partial labeling scheme is shown in Figure 1. Selected bond distances and angles are collected in Table 2. Both Ni(II) ions in **2** are six coordinate and are each bound to two benzimidazole ring nitrogen atoms, one amine nitrogen atom, an ether oxygen atom, and two acetonitrile nitrogen atoms. The Ni(II) ions are tethered together by a diethyl ether linkage with a crystallographic center of inversion between the methylene carbons of this bridge. The centrosymmetric nature of **2** requires that the Ni−OCH_2CH_2O−Ni torsion angle be 180°. This crystallographically imposed symmetry also requires that each Ni ion reside in identical sites. The Ni atom adopts a distorted octahedral geometry and sits 0.228 Å below the plane of N11, N4, N21, and O1 in the direction of the acetonitrile ligand nitrogen N3. This geometry is in fact required by the tetrapodal chelating ligand and the nearly perfect tetrahedral geometry about the tertiary amine nitrogen N1. Therefore, the benzimidazole nitrogens N11 and N21 coordinate facially to the Ni(II) ion along with the amine nitrogen N1. This places the amine nitrogen trans to an acetonitrile ligand and the ether oxygen O1 trans to the benzimidazole nitrogen N11.

Table 2. Selected Bond Lengths and Bond Angles for $[Ni_2(EGTB\text{-}Et)(CH_3CN)_4](ClO_4)_4\cdot 2CH_3CN$[a]

Bond Lengths (Å)			
Ni−N(1)	2.128(7)	Ni−O(1)	2.101(6)
Ni−N11	2.058(6)	Ni−N21	2.046(5)
Ni−N3	2.052(8)	Ni−N4	2.108(6)
Bond Angles (deg)			
N1−Ni−O1	80.6(2)	N(1)−Ni−N11	79.6(3)
O1−Ni−N11	158.1(3)	N1−Ni−N21	82.2(2)
O1−Ni−N21	88.7(2)	N11−Ni−N21	97.7(2)
N1−Ni−N3	177.0(3)	O1−Ni−N3	96.9(2)
N11−Ni−N3	103.2(3)	N21−Ni−N	96.1(3)
N1−Ni−N4	93.3(3)	O1−Ni−N4	83.4(2)
N11−Ni−N4	88.6(2)	N21−Ni−N4	171.5(3)
N3−Ni−N4	88.0(3)		

[a] For labels, see ORTEP drawing.

The average Ni−N distance (2.078 Å) in **2** are typical of Ni−N distances of several crystallographically characterized Ni(II) complexes (Table 2).[24−32] The longest nickel−nitrogen bond length in **2** is 2.128 Å and is trans to the acetonitrile ligand N3 (2.052 Å). This difference in bond length is likely due to the difference in ligand basicity between the tertiary amine and the acetonitrile ligand. This basicity difference is also reflected in the Ni−N4 and the Ni−N21 bond distances. The more basic benzimidazole nitrogen N21 has a bond length of 2.046 Å while the Ni−N4 acetonitrile bond length is 2.108 Å. Similarly, the benzimidazole nitrogen N11 is trans to the ether oxygen O1, and the metal−ligand bond distances are 2.058 and 2.101 Å, respectively. The N11−Ni−O1 bond angle is 158.1° reflecting a much larger distortion in the Ni(II) octahedron. This is also evident in the N1−Ni−O1 and N21-Ni−O1 bond angles which are 80.6 and 88.7°, respectively. The deviation of these angles from the idealized (90°) for octahedral symmetry, is due to the subtle interplay of basicity arguments and the fact that only five member chelate rings occur in this complex. The Ni--Ni separation in **2** is 7.072 Å, making it one of the longest for a dinuclear Ni(II) complex.

X-ray diffraction studies were also carried out on $[Ni(Bipy)_2(OAc)](ClO_4)\cdot 2H_2O$ (**3**). Compound **3** crystallizes in the monoclinic space group $P2_1/c$. Two $[Ni(Bipy)_2(OAc)]^+$ cations are found in the unit cell along with one perchlorate and two water molecules. The Ni(II) ion lies on a crystallographic center of inversion. The space group $P2_1/c$ allows the two expected optical isomers of **3** to be present in the crystal lattice. A packing diagram indicates that the cations of **2** are layered in

(24) Urtiaga, M. K.; Pizarro, J. L. *Acta Crystallogr.* **1994**, *C50*, 56−58.
(25) Buchanan, R. M.; Mashuta, M. S.; Oberhausen, K. J.; Richardson, J. F. *J. Am. Chem. Soc.* **1989**, *111*, 4497−4498.
(26) Holman, T. R.; Hendrich, M. P.; Que, L. J. *Inorg. Chem.* **1992**, *31*, 937−939.
(27) Nanda, K. K.; Das, R.; Thompson, L. K.; Venkatsubramanian, K.; Nag, K. *Inorg. Chem.* **1994**, *33*, 5934−5939.
(28) Turpeinen, U.; Hämäläinen, R.; Reedijk, J. *Polyhedron* **1987**, *6*, 1603−1610.
(29) Ahlgren, M.; Turpeinen, U.; Hämäläinen, R. *Acta Chem. Scand. A* **1978**, *32*, 189−194.
(30) Wages, H. E.; Taft, K. L.; Lippard, S. J. *Inorg. Chem.* **1993**, *32*, 4985−4987.
(31) Chaudhuri, P.; Küooers, H.-J.; Wieghardt, K.; Gehring, S.; Haase, W.; Nuber, B.; Weiss, J. *J. Chem. Soc., Dalton Trans.* **1988**, 1367−1370.
(32) Stemmler, A. J.; Kampf, J. W.; Kirk, M. L.; Pecoraro, V. L. *J. Am. Chem. Soc.* **1995**, *117*, 6368−6369.

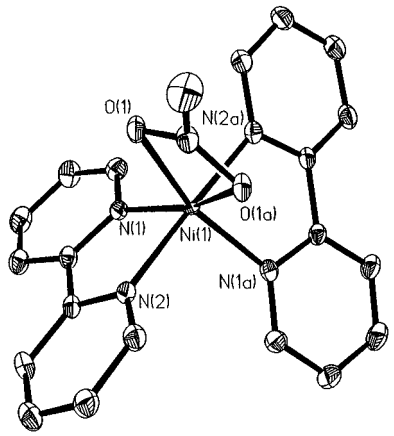

Figure 2. ORTEP drawing of the $[Ni(bipy)_2(OAc)]^+$ cation showing a partial numbering scheme (carbon and hydrogen atoms are not labeled for clarity).

Table 3. Selected Bond Lengths and Bond Angles for $[Ni(Bipy)_2(OAc)]ClO_4 \cdot 2H_2O$[a]

	Bond Lengths (Å)		
Ni1−O1	2.110(3)	Ni1−N1A	2.067(3)
Ni1−N1	2.067(3)	Ni1−N2	2.056(4)
Ni1−O1A	2.110(3)	Ni1−N2A	2.056(4)
	Bond Angles (deg)		
N1−Ni−N2	79.4(1)	O1−Ni−N1	98.4(1)
N1−Ni−N1A	101.1(2)	O1−Ni−N2	91.2(1)
N1−Ni−N2A	96.4(1)	O1−Ni−N1A	160.1(1)
N1−Ni−O1A	160.1(1)	O1A−Ni−N1A	98.4(1)
N1A−Ni−N2A	79.4(1)	O1−Ni−N2A	94.5(1)
N2−Ni−N1A	96.4(1)	O1A−Ni−N2A	91.2(1)
N2−Ni−N2A	173.4(2)	O1−Ni−O1A	62.5(1)
N2−Ni−O1A	94.5(1)		

[a] For labels, see ORTEP drawing.

between perchlorate anions (see Supporting Information). In addition, two water molecules are present in the crystal lattice and form hydrogen bonds with adjacent para- and meta-hydrogen atoms of a single bipyridine ring. A thermal ellipsoid drawing of the cation of **3** with a partial labeling scheme is shown in Figure 2. Selected bond distances and angles are collected in Table 3.

The Ni(II) ion in **3** adopts a distorted octahedral geometry and is bound to four bipyridine ring nitrogen atoms, and two carboxylate oxygen atoms. The average Ni−N and Ni−O distances are 2.062 and 2.110 Å (Table 3). These bond distances are comparable to distances reported for other crystallographically characterized nickel−pyridine and nickel carboxylate complexes.[24−32] The N1−Ni−N2 bond angle is 79.4° and the O1−Ni−O1A bond angle is 62.5°. The small bite angle of the bipyridine and carboxylate ligands result in very acute bond angles for an octahedral geometry. This distortion is also reflected in the bond angles between the trans ligands. The N1−N4−O1A bond angle is 160.1 compared to 173.4 for the N2−Ni−N2A bond angle. The deviation of these angles from the idealized octahedral geometry is also due to the fact that a four-member chelate rings occurs for the chelated carboxylate while bipyridine forms five-member chelate rings. Therefore, small bite angles for bipyridine and the carboxylate ligand as well as four- and five-member chelate rings provide a very distorted Ni(II) octahedron for **3**. Another Ni(II) bypyridine complex $[Ni(Bipy)_2(NCO)_2]$ was recently crystallographically characterized and is very similar to **3**, except for the distortions imposed by the chelated carboxylate moiety.[24]

Electronic Absorption Spectra. The electronic absorption spectra for **2** and **3** in acetonitrile solution are shown in Figure 3. All of the complexes studied exhibited absorptions in the 200−350 nm range that can be attributed to ligand absorption bands and/or ligand-to-metal charge transfer bands (LMCT). As expected for high-spin octahedral Ni(II) complexes, spin allowed d−d bands are observed in the 450−1000 nm range. For **2**, two broad absorptions are observed at 586 nm ($\epsilon = 14$ M^{-1} cm^{-1}) and 925 nm ($\epsilon = 14$ M^{-1} cm^{-1}) that are assigned to the $^3A_{2g} \rightarrow {}^3T_{1g}(F)$ and $^3A_{2g} \rightarrow {}^3T_{2g}(F)$ transitions, respectively. A weak absorption band at 810 nm ($\epsilon \sim 8$ M^{-1} cm^{-1}) is due to the spin-forbidden $^3A_{2g} \rightarrow {}^1E_{1g}$ transition. However, the third d−d band ($^3A_{2g} \rightarrow {}^3T_{1g}$ (P)), expected for d^8 octahedral Ni(II) complexes between 350 and 420 nm, is not observed due to overlap with a $\pi-\pi^*$ transition of the benzimidazole ring or a benzimidazole nitrogen-to-Ni(II) LMCT band. Similarly, two absorption bands at 557 nm ($\epsilon = 25$ M^{-1} cm^{-1}) and 877 nm ($\epsilon = 16$ M^{-1} cm^{-1}) are observed for **3** and are assigned to the $^3A_{2g} \rightarrow {}^3T_{1g}(F)$ and $^3A_{2g} \rightarrow {}^3T_{2g}(F)$ transitions, respectively. A weak absorption band at 790 nm ($\epsilon \sim 12$ M^{-1} cm^{-1}) is also observed for **3** and can be assigned to the spin-forbidden $^3A_{2g} \rightarrow {}^1E_{1g}$ transition. Inspection of the Tanabe−Sugano energy level diagrams for a d^8 octahedral system provides crystal field splitting parameters of 1081 and 1140 cm^{-1} and Racah parameters of approximately 840 and 820 cm^{-1} for **2** and **3**, respectively. These values compare well with those for other high-spin octahedral Ni(II) complexes as well as urease (407, 745, and 1060 nm) and carboxypeptidase A (412, 685, 1060 nm).[11,33,34]

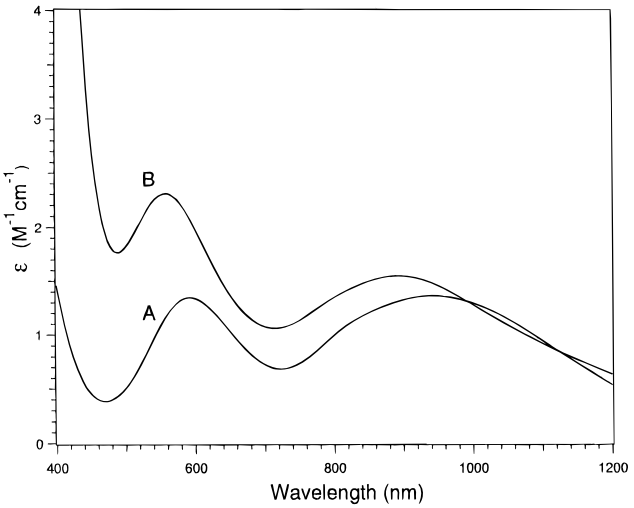

Figure 3. Visible electronic absorption spectra: (A) $[Ni_2(EGTB\text{-}Et)(CH_3CN)_4]^{4+}$ and (B) $[Ni(bipy)_2(OAc)]^+$ in acetonitrile solution.

^{1}H NMR Studies. ^{1}H NMR spectra of **2** and **3** at 40 and 10 °C, respectively, in acetonitrile solution are shown in Figure 4 , and relevant data are gathered in Table 4. Both complexes exhibit several sharp hyperfine-shifted ^{1}H NMR signals that sharpen and shift toward the diamagnetic region as the temperature is increased, following Curie law behavior (see Supporting Information). Inspection of these two spectra reveal that the overall chemical shift of **2** compared to **3** is markedly less. For **2**, several isotropically shifted signals are observed at 40 °C in acetonitrile solution in the 35−0 ppm chemical shift range; however, **3** exhibits hyperfine shifted signals in acetonitrile solution at 10 °C in the 175−0 ppm chemical shift region. The greater isotropic shift observed for **3** is similar to Ni(II) ions in tetrahedral environments.[1] However, from electronic

(33) Blakeley, R. L., Dixon, N. E., and Zerner, B. *Biochim. Biophys. Acta* **1983**, *744*, 219−229.
(34) Rosenberg, R. C.; Root, C. A.; Gray, H. B. *J. Am. Chem. Soc.* **1975**, *97*, 21−26.

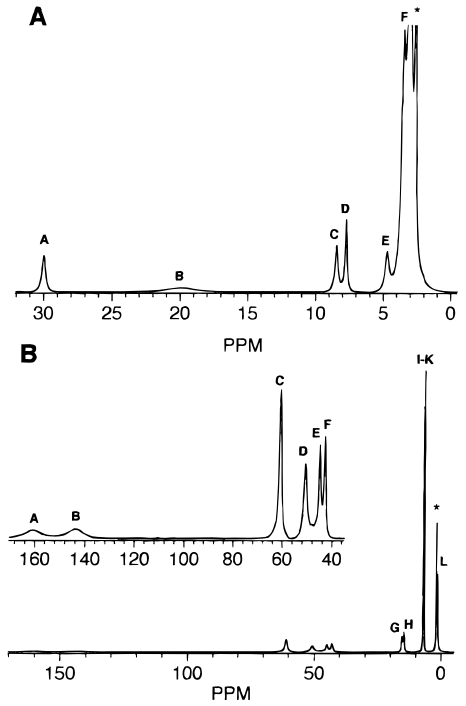

Figure 4. ^{1}H NMR spectra: (A) spectrum of **2** in CD_3CN at 40 °C and (B) spectrum of **3** in CD_3CN at 10 °C. Spectrum was referenced to the residual protic solvent signals (*) at 2.26 and 1.92 ppm for water and acetonitrile.

absorption spectroscopy it is clear that the Ni(II) ion in **3** retains its octahedral coordination geometry in acetonitrile solution. Therefore, on the basis of the X-ray structure of **3**, the distortions in the octahedron due to the small bite angle of the chelated carboxylate moiety (62.5°) and the Bipy ligand (79.4°) (Figure 2, Table 3), result in a larger magnetic anisotropy that in turn induces a larger dipolar shift.[1] These data reaffirm the limited nature of ^{1}H NMR spectra for the determination of coordination numbers for Ni(II) centers.

Initial assignments of several isotropically shifted ^{1}H NMR signals for **2** can be made by inspection of their peak areas and T_1 values (Table 4). Signals A (30 ppm; 7 ms), C (8.4 ppm; 5 ms), and D (7.6 ppm; 11 ms) integrate to four protons each. These data taken together with the crystallographic data suggest that these four signals are due to the benzimidazole ring protons. The remaining signals are B (20 ppm; 1 ms), E (4.6 ppm; 3 ms), F (3.5 ppm; 5 ms), and G (2.5 ppm). Integration of signals F and G is difficult due to overlap with the residual solvent (H_2O and CH_3CN) signals. From the X-ray crystallographic data, relatively sharp isotropically shifted ^{1}H NMR resonances are expected only from the N-alkylated ethylene protons and the diethyl ether CH_2-CH_2 bridge. Therefore, signals E and G are tentatively assigned to the CH_3-CH_2 protons of the N-alkylated ethylene protons, respectively. Signal F is tentatively assigned to the diethyl ether CH_2-CH_2 moiety since the X-ray structure of **2** reveals a center of symmetry between these two carbons likely causing the methylene CH_2 protons to resonate at similar frequencies. The broad signal B is tentatively assigned to either the benzimidazole α-H protons or the methylene CH_2 protons of the EGTB-Et ligand.

Definitive assignment of the observed isotropically shifted signals comes from two-dimensional ^{1}H NMR techniques. A magnitude COSY spectrum of **2**, recorded at 40 °C, clearly shows cross signals between resonances A and D and also between resonances C and D (Figure 5). These signals are unequivocally assigned to the benzimidazole β-H (A or C), β'-H (A or C), and γ-H (D) protons, respectively (EGTB-Et; **1**). In addition, a clear cross signal is observed between resonances E and G (Figure 5). These resonances can be assigned to the CH_3-CH_2 protons of the N-alkylated ethylene protons, respectively. The only remaining unassigned resonances are at 20 (B) and 3.5 ppm (F). The close proximity of the methylene CH_2 protons of **2** to the Ni(II) centers (>3 Å) likely cause their isotropically shifted resonances to be broadened beyond detection. On the basis of T_1 values, signal B (1 ms) is assigned to the benzimidazole α-H protons which are >5 Å from the Ni(II) center while F (5 ms) is assigned to the diethyl ether CH_2-CH_2 protons.

The ^{1}H NMR spectrum of **3** reveals isotropically shifted signals in the 175−0 ppm chemical shift range at 10 °C in acetonitrile solution (Figure 4). On the basis of the X-ray crystallographic results for **3**, the pyridine groups of the Bipy ligand are in distinct environments. The maximum number of hyperfine shifted ^{1}H NMR signals expected for **3** would be nine; however, 12 isotropically shifted signals are observed. Since the electronic absorption spectrum of **3** is consistent with an octahedral geometry in acetonitrile solution, a coordination number change to five or four can be ruled out. The fact that additional signals are observed suggests that the two optical isomers of **3** are resolved in the ^{1}H NMR spectrum. A maximum of 18 isotropically shifted signals would then be expected. If a predominantly contact shift interaction is assumed[1] and the distortions of **3** away from an idealized octahedral coordination geometry are considered, the axial pyridine ring protons would be expected to have a larger isotropic shift then the equatorial pyridine protons. Similar results for Ni(II) complexes with pyridine ligands have been previously reported.[35]

Several of the isotropically shifted ^{1}H NMR signals observed for **3** can be initially assigned by substitution and inspection of their peak areas. Addition of [D_3]acetate to **3** causes signals D (51 ppm) and F (43 ppm) to disappear. ^{2}H NMR experiments confirm these assignments. These data taken together with the integrations, line widths, and T_1 values of D and F indicate that these two resonances are due to the acetate methyl protons of the two optical isomers of **3**. Since urease and AAP contain coordinated carboxylate residues, the chemical shift of the CH_3 protons in **3** provides essential chemical shift information for these types of protons. Signals E (45 ppm), G (15.3 ppm), H (14.6 ppm), I (7.3 ppm), J (7.0 ppm), and K (6.8 ppm) integrate to approximately two protons each (Table 4). These data, taken together with the crystallographic results and the fact that two isomers exist in solution, suggest that signals E, G, and H may arise from equatorial pyridine ring protons of a coordinated Bipy for one isomer while signals I, J, and K likely arise from equatorial pyridine ring protons of the second isomer. Of the remaining signals, A (160 ppm), B (144 ppm), and C (61 ppm) all integrate to approximately four protons each. These resonances are tentatively assigned to the remaining pyridine ring protons of both isomers. The only protons that are unaccounted for are the pyridine α-H protons. Since these protons will be >3 Å for the Ni(II) center, their isotropically shifted resonances will likely be broadened beyond detection.

Definitive assignment of several of these signals comes from two-dimensional ^{1}H NMR techniques. A magnitude COSY spectrum of **3** was recorded at 10 °C and clearly shows cross signals between resonances I and J and also between resonances J and K (Figure 6). These signals can be assigned to the equatorial pyridine β-H (I or K), β'-H (I or K), and γ-H (J) protons, respectively, of a coordinated Bipy ligand. In addition, cross signals are observed between signals G and H. These

(35) La Mar, G.; Sacconi, L. *J. Am. Chem. Soc.* **1967**, *89*, 2282−2291.

Table 4. ^{1}H NMR Chemical Shifts for $[Ni_2(EGTB\text{-}Et)(CH_3CN)_4]^{4+}$ and $[Ni(Bipy)_2(OAc)]^+$ in CD_3CN Solution at 40 and 10 °C, respectively

	$Ni_2(EGTB\text{-}Et)(CH_3CN)_4]^{4+}$					$[Ni(Bipy)_2(OAc)]^+$				
	assign	chem shift[a]	rel area	line width[b] (Hz)	T_1[c] (ms)	assign	chem shift[a]	rel area	line width[b] (Hz)	T_1[c] (ms)
A	Bz β-**H**	30	4	140	7	Py β'-**H**	160	4	~3100	~1
B	Bz α-**H**	20	~4	950	1	Py β-**H**	144	4	~2900	~1
C	Bz β'-**H**	8.4	4	110	5	Py γ-**H**	61	4	460	2
D	Bz γ-**H**	7.6	4	90	11	C**H**$_3$	51	3	600	2
E	C**H**$_3$CH$_2$	4.6	8	160	3	Py β'-**H**	45	2	425	3
F	C**H**$_2$	3.5		150	5	C**H**$_3$	43	3	400	3
G	CH$_3$C**H**$_2$	~2.5				Py γ-**H**	15.3	2	300	7
H						Py β-**H**	14.6	2	250	7
I						Py β-**H**	7.3	2	45	82
J						Py γ-**H**	7.0	2	45	66
K						Py β'-**H**	6.8	2	60	78

[a] All shifts are in ppm relative to the residual solvent signal at 1.92 ppm. [b] The line widths are full width at half-maximum. [c] T_1 values were obtained at 400 MHz.

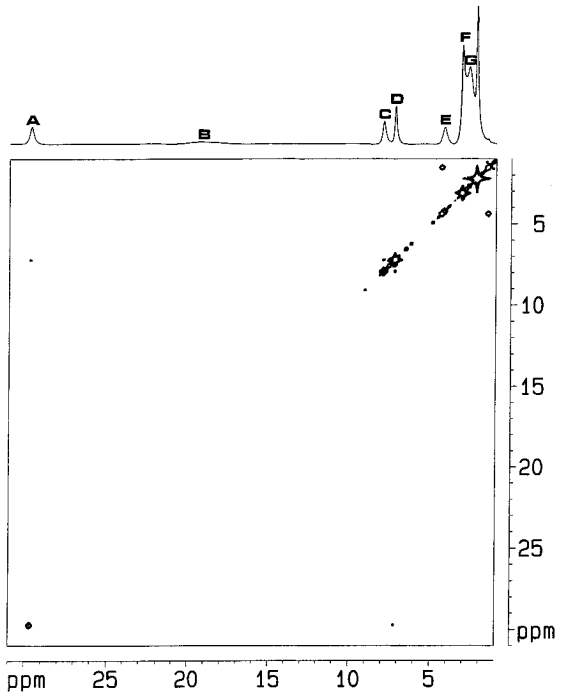

Figure 5. Magnitude ^{1}H COSY spectrum of **2** obtained at 400.17 MHz (Bruker ARX-400) at 40 °C in CD_3CN solution. Spectrum was referenced to the residual protic solvent signals (*) at 2.26 and 1.92 ppm for water and acetonitrile. This spectrum was obtained with an acquisition time of 35 ms and 512 data points in the F1 dimension and 1024 data points in the F2 dimension. An unshifted sine-bell squared weighting function and zero-filling to 2048 data points were applied prior to Fourier transformation in both dimensions.

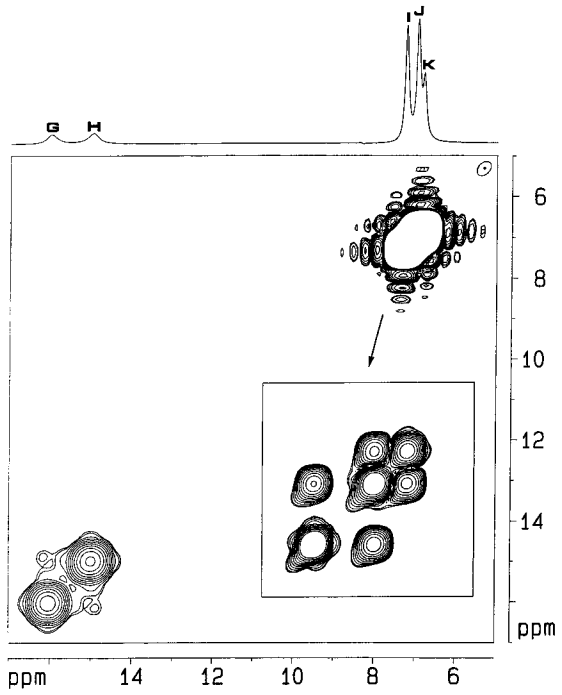

Figure 6. Magnitude ^{1}H COSY spectrum of **3** obtained at 400.17 MHz (Bruker ARX-400) at 10 °C in CD_3CN solution. This spectrum was obtained with an acquisition time of 8 ms and 256 data points in the F1 dimension and 512 data points in the F2 dimension. An unshifted sine-bell squared weighting function and zero-filling to 1024 data points were applied prior to Fourier transformation in both dimensions. Inset: Expanded view of the 8−6 ppm portion of a Magnitude COSY spectrum of **3** highlighting the cross signals for I and J and also for J and K. This spectrum was obtained with an acquisition time of 60 ms and 512 data points in the F1 dimension and 1024 data points in the F2 dimension. An unshifted sine-bell squared weighting function and zero-filling to 2048 data points were applied prior to Fourier transformation in both dimensions.

protons are assigned to the β-H, and γ-H protons of a second pyridine group of a Bipy ligand. While a definitive COSY cross-signal was not observed between signals E (3 ms) and G (7 ms) due to their large line widths, signal E is assigned to the remaining β-H proton based on its line width and integration. Signals A (160 ppm; ~1), B (144 ppm; ~1), and D (57 ppm; 2) are the only remaining unassigned signals in the ^{1}H NMR spectrum of **3**. The only protons in **3** not assigned are the pyridine α-H protons and the pyridine β'-H protons of the two inequivalent pyridine rings.

Conclusion

We have synthesized and crystallographically characterized a new dinickel(II) complex that contains a diethyl ether moiety bridging between the two Ni(II) ions with terminal benzimidazole, amine nitrogen, and acetonitrile ligands. The diethyl ether bridge results in a long (7.072 Å) Ni−Ni separation that prevents any magnetic coupling between the two Ni(II) ions. In addition, a new mononuclear Ni(II) complex with a chelated acetate group and bypyridine ligands has been synthesized and crystallographically characterized. Both of these complexes have been spectroscopically characterized in acetonitrile solution by electronic absorption and two-dimensional (COSY) ^{1}H NMR methods. From the COSY data, the solution structures of both **2** and 3 are consistent with the X-ray crystallographic results. The ^{1}H NMR spectrum of **3** also resolves the two optical isomers of **3** and provides important chemical shift information for coordinated carboxylate groups residing in metalloprotein active sites. The use of 2D NMR methods to assign inequivalent aromatic protons, rather than synthetic methods such as substitution or deuteration, greatly simplifies the structural characteriza-

tion of paramagnetic model complexes in solution. Studies of this type on the hyperactive dinuclear Ni(II)-substituted AAP enzyme are currently in progress.

Acknowledgment. This work was supported by the National Science Foundation (Grant CHE-9422098) and the Petroleum Research Fund (Grant ACS-PRF 28635-G). The Bruker ARX-400 NMR spectrometer was purchased with funds provided by the National Science Foundation (CHE-9311730) and Utah State University. We acknowledge the NSF for partial funding of the X-ray diffractometer (Grant CHE-9002379). The authors are grateful to Professor John L. Hubbard for his assistance in the crystal structure determinations and to Ms. Julie M. Brink, and Mr. Daniel B. Falk for helpful discussions.

Supporting Information Available: Tables detailing the X-ray data collection and refinement, crystal packing diagrams, tables of atomic coordinates, bond distances, bond angles, final anisotropic thermal parameters, and calculated or refined H atom coordinates, and isotropic shift vs $1/T$ plots for both **2** and **3** (16 pages). Ordering information is given on any current masthead page.

IC951106B